

## Stresses in ultrasonically assisted bone cutting

This content has been downloaded from IOPscience. Please scroll down to see the full text.

2009 J. Phys.: Conf. Ser. 181 012014

(<http://iopscience.iop.org/1742-6596/181/1/012014>)

View [the table of contents for this issue](#), or go to the [journal homepage](#) for more

Download details:

IP Address: 124.160.105.200

This content was downloaded on 14/07/2016 at 07:16

Please note that [terms and conditions apply](#).

## Stresses in ultrasonically assisted bone cutting

K Alam<sup>1</sup>, A V Mitrofanov<sup>1</sup>, M Bäker<sup>2</sup> and V V Silberschmidt<sup>1</sup>

<sup>1</sup> Wolfson School of Mechanical and Manufacturing Engineering, Loughborough University, UK

<sup>2</sup> Institut für Werkstoffe, Technische Universität Braunschweig, Langer Kamp 8, 38106 Braunschweig, Germany

Email: k.alam2@lboro.ac.uk

**Abstract.** Bone cutting is a frequently used procedure in the orthopaedic surgery. Modern cutting techniques, such as ultrasonic assisted drilling, enable surgeons to perform precision operations in facial and spinal surgeries. Advanced understanding of the mechanics of bone cutting assisted by ultrasonic vibration is required to minimise bone fractures and to optimise the technique performance. The paper presents results of finite element simulations on ultrasonic and conventional bone cutting analysing the effects of ultrasonic vibration on cutting forces and stress distribution. The developed model is used to study the effects of cutting and vibration parameters (e.g. amplitude and frequency) on the stress distributions in the cutting region.

### 1. Introduction

Understanding the mechanical behaviour of bones that leads to their failure is necessary for diagnosis and prevention of bone fracture and diseases. Knee and hip implant surgeries are performed around the world and are considered the most common operations in clinical practice. A total of 300,000 knee arthroplasties are performed each year in the United States alone with the number increasing every year [1]. For years, researchers have employed mechanical testing and finite element (FE) models to study how and why bone fractures under various loading conditions [2,3,4,5]. Bone has a capability to adapt to its mechanical environment and to reconstruct functionally its structure and geometry [6,7]. One of the important mechanical factors affecting bone remodelling is the stress in bone tissue. For remodelling to occur, bone should possess some stress present in its tissue to stimulate the osteocyte over a relatively long period. This stress will be a type of residual stress that satisfies the force equilibrium condition in the bone material [8,9].

Bone is subjected to stresses in cutting processes which are the essential part of any orthopaedic surgery. Limited studies have been performed to measure the level of stresses in bone cutting. In [10], the chip generation process was observed under an optical microscope while cutting pig cortical bone – i.e. the hard outside layer of the long bone such as femur or tibia. The measured shear angle was approximately 27° for all tool rake angles, and continuous type cutting chips were generated. The shear stress was approximately 40 MPa independent of the tool rake angle. The shear stress on the shear plane was decreased with an increase in the tool rake angle and was found to depend on cutting orientation. A FE analysis of bone cutting has not been reported in literature so far due to unavailability of correct material properties for such modelling and difficulties inherent to numerical modelling of material separation.

Several modern bone cutting techniques were introduced that aim at minimizing the invasiveness and improving the safety of the operation. Ultrasonically assisted bone cutting (UAC) is one of such techniques. UAC has been previously utilized in cutting super alloys, composites, food and biomaterials [11,12]. In UAC, a high-frequency vibration (frequency 10-50 kHz, amplitude 10-30  $\mu\text{m}$ ) is superimposed on the movement of a cutting tool (see figure 1). Compared to conventional cutting (CC), this technique results in a decrease in the cutting force and an improvement in the surface finish [13]. Dynamics of UAC as a non-linear vibro-impact process was studied in [14] and the amplitude response of the cutting tool under loading was analysed for this cutting technique. However, the influence of UAC on the material behaviour in bone cutting has not been studied yet.

Analysis of the mechanics of cutting and its effect on stress distributions in the bone tissue would facilitate optimal prosthesis design and fabrication. This may also be helpful in reducing the risk of mechanical failures and in improving bone-implant longevity. In bone cutting, two types of stresses are necessary to be measured: (1) stresses generated during the chip formation which affect cutting mechanics and (2) residual stresses that are important for the bone-implant interface strength. The current work is aimed at investigating the level of stresses induced in bone when a hard cutting tool penetrates into it in the ultrasonically assisted/vibratory mode. Calculated stresses are compared with those generated in the conventional cutting mode. The effect of ultrasonic frequency and amplitude on material stresses is discussed. The model allows us to study the bone-tool interaction in vibratory mode, hence enabling the optimization / evaluation of the cutting procedure.

## 2. FE model description

The MSC.Marc general FE code [15] was used in the development of our two-dimensional FE model of bone cutting. A rectangular part of the bone was modelled with dimensions of 2 mm  $\times$  1 mm. The work piece was modelled with four-node, isoparametric, arbitrary quadrilateral elements and assuming plane-strain conditions. The cutting tool was modelled with rigid lines as the stiffness of the tool material was much greater than that of the bone.

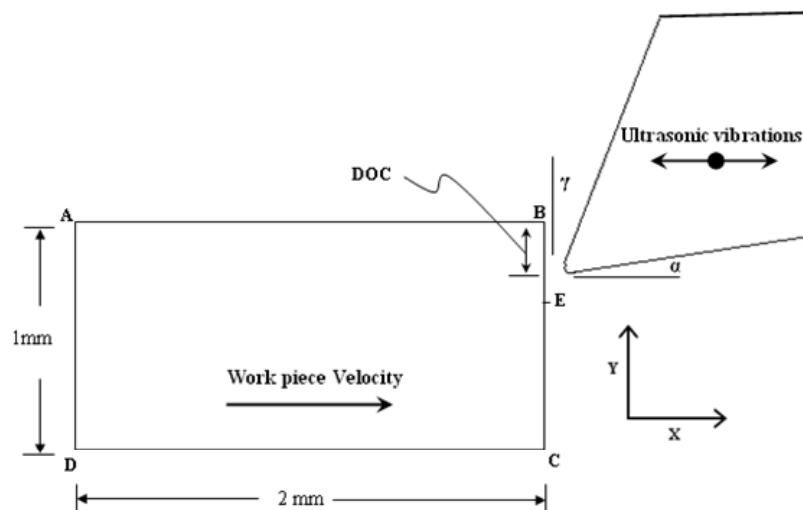


**Figure 1.** Scheme of the relative movement of the work piece and tool in UAC.

In simulations of UAC, the work piece was moved with a constant velocity in the  $X$ -direction, and the tool was vibrated with the required frequency and amplitude. In conventional cutting (CC), the tool position was fixed, and the workpiece was advanced with the constant velocity as before. Remeshing was applied every 10 increments in simulations to avoid convergence issues associated with highly distorted elements. The effect of remeshing frequency on magnitudes of the calculated force and stresses was negligible. Increasing the remeshing frequency significantly increased the analysis time. A contact was defined between the tool and the workpiece, where relative motion between them was allowed under friction conditions. A shear friction model frequently used for modelling of cutting processes was chosen for simulations. The software [15] used in simulations has the capability to detect the contact automatically. To check the contact stability in the iteration process, the motion of the node was controlled with regard to its penetration of a surface by a certain amount.

The developed FE model was fully thermo-mechanically coupled in order to properly reflect interconnection between thermal and mechanical processes. The FE model presupposes formation of the continuous chip, which is in a good agreement with the results of our high-speed filming experiments of bone drilling and other results reported [16,17]. All the simulations were continued until full chip formation was achieved, i.e. cutting forces, stresses and strains reached their saturated levels.

## 2.1. Material data

The bone tissue is a heterogeneous material with complex multi-level microstructure that is approximated in this paper with an equivalent homogeneous material (EHM). An elastic modulus of bone was measured from the nanoindentation test and incorporated into the FE model. Material separation ahead of the tool occurred when the breaking stress (obtained from the tensile test) was reached. The Johnson-Cook (JC) material model [12, 18] that accounts for the strain rate sensitivity and temperature effects was utilised for the bone tissue as it allowed an accurate approximation of our experimental data. In this model, the bone is considered as an elastic-plastic material with nonlinear strain hardening:

$$\sigma_y = \left( A + B \varepsilon_p^n \right) \left( 1 + C \ln \left( \frac{\dot{\varepsilon}_p}{\dot{\varepsilon}_o} \right) \right) (1 - T^{*m}) \quad (1)$$

where  $A$ ,  $B$ ,  $C$  and  $n$  are constants and  $T^* = \frac{(T - T_{\text{room}})}{(T_{\text{melt}} - T_{\text{room}})}$ ;

$\varepsilon_p$  and  $\dot{\varepsilon}$  are the plastic strain and strain rate, respectively;  $T_{\text{room}}$  and  $T_{\text{melt}}$  are the room and melting temperatures, respectively; the term  $T^*$  was omitted in simulations at this stage of investigations. The JC constants are calculated by fitting the equation into the stress-strain graphs for different load rates obtained from our experimental tensile tests on the bone. Their magnitudes used in the simulations are given in table 1. Other material properties were taken from literature and are provided in table 2.

**Table 1.** Johnson-Cook parameters used in cutting simulations.

$A$ (MPa)	$B$ (MPa)	$C$	$n$
50	101	0.03	0.08

**Table 2.** Material properties of bone used in simulations

Property name	Value	Reference
Elastic modulus	20 GPa	measured
Density	$2.26 \times 10^3 \text{ kg/m}^3$	[19]
Thermal conductivity	0.2, 0.53 W/m K	[20, 21]
Specific heat	1.26 kJ/kg K	[19]

## 2.2. Boundary conditions

Constraints on the elements were not feasible in simulations with remeshing due to the software limitations. To resolve this, rigid lines AD, DC and CE (shown in figure 1) were created at the left, bottom and right edges of the work piece and were permanently glued to it. Kinematic boundary conditions were applied at these lines, which were transferred to the work piece elements. The cutting tool was vibrated harmonically in the cutting direction given by equation (2)

$$u_x = -a \cos \omega t, \quad u_y = 0, \quad (2)$$

where  $u$  is the tool displacement,  $\omega = 2\pi f$  is angular frequency,  $f$  is vibration frequency and  $a$  is amplitude. For the frequency and amplitude chosen for simulations, the linear velocity of the tool was higher than the cutting velocity (i.e. the velocity of the work piece). This led to the intermittent contact condition between the tool and work piece. Analyses were run assuming dry cutting conditions, i.e. cutting without irrigation.

## 2.3. Cutting parameters

In simulations, various parameters, such as the ultrasonic amplitude, frequency and cutting velocity were changed to observe their effect on stresses. Cutting parameters and their magnitudes used in simulations are given in table 3.

**Table 3.** Cutting parameters used in simulations of the bone cutting process.

Parameters	Magnitudes, used in FEA
Cutting speed (mm/sec)	100; 150; 200; 250; 300
Friction coefficient	0.3
Tool nose radius ( $\mu\text{m}$ )	10
Tool rake angle, $\gamma$ (deg)	15
Amplitude ( $\mu\text{m}$ )	10; 15; 20; 30
Frequency (kHz)	10; 20; 30

## 3. Results

Simulations were run from the initial contact between the cutting tool and workpiece until a state of the fully formed chip. The stress distribution in the bone material changed with the penetration depth and achieved a stable value exceeding the material yield limit when the chip was formed. The increase in stress levels beyond the yield strength of the material is due to strain hardening. The separation of the

material in the cutting process occurs in the vicinity of the cutting edge that moves along the prescribed straight line in the simulations. The material fails when the stress in it exceeds the critical value.

### 3.1. Stress calculations

To estimate the level of stresses induced by the tool in the bone tissue, simulation results obtained for UAC were compared to those of CC for identical cutting conditions. The simulations were performed with various cutting speeds as given in table 3; in other case studies the level of 300 mm/s was used. In CC, the stress reached almost a constant value of 140 MPa at 0.7 ms and remained stable for the remaining cut (up to full chip formation). At the initial stage of cutting, stresses were relatively small and concentrated around the tool tip in both the chip and machined surface. As the cutting process continued until the shear band was fully formed, the deformation increased and spread over a zone where shear banding takes place. The deformation zones produced in the material when the tool advanced are shown in figure 2; they are characterised by high levels of stresses (bright colours in the figure). It was noticed that the field of maximum shear stress is almost the same in primary and secondary deformation zones. The maximum equivalent stress fluctuated between 135-142 MPa and the measured shear angle was approximately  $40^\circ$ . The stress fluctuation can be attributed to numerical errors inherent to finite element simulations as well as to the frequent remeshing scheme.

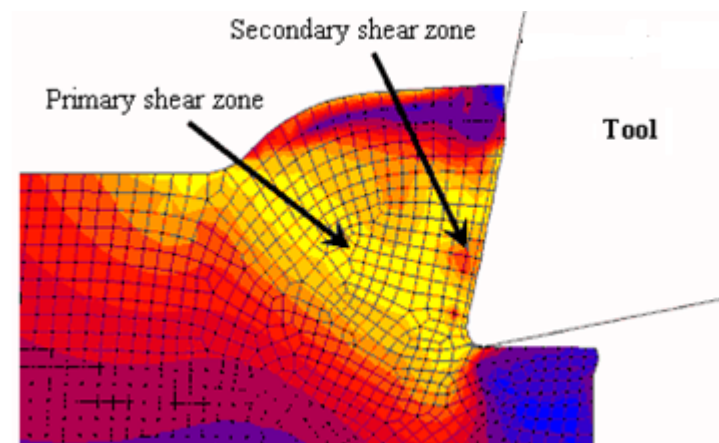


**Figure 2.** Deformation zones produced when tool penetrated into material in conventional cutting of bone (cutting speed 300 mm/s)

To fully understand the material's response in the interaction with the ultrasonic tool, the stress variation with tool motion is split into two stages: (a) when the tool penetrated into the material in the forward direction (b) when the tool travelled away from the chip. In UAC, during the continuous chip formation, a dynamically changing stress distribution in the process zone was observed. Figure 3 shows characteristic stages of a single cycle of vibration that took about 0.05 ms. When the tool moved forward, the stress increased with tool penetration and attained a maximum value of approximately 140 MPa. The attainment of the maximum penetration depth was characterized by the highest levels of generated stresses in the process zone and indicated the end of loading/penetration stage (figure 3a). When the tool moved in the opposite direction, the level of maximum stress dropped to an average value of 30 MPa (figure 3b). Those were the residual stresses induced in the material due to its plastic deformation. During each cycle cutting force increased in the same fashion and achieved a peak value at maximum penetration depth (end of loading) as shown in figure 4. The force dropped as the tool started moving away from the work piece

and eventually vanished when separated from it. The maximum stress values were almost the same for all loading/cutting stages in UAC. As these maximum stresses were reached only during the loading part of

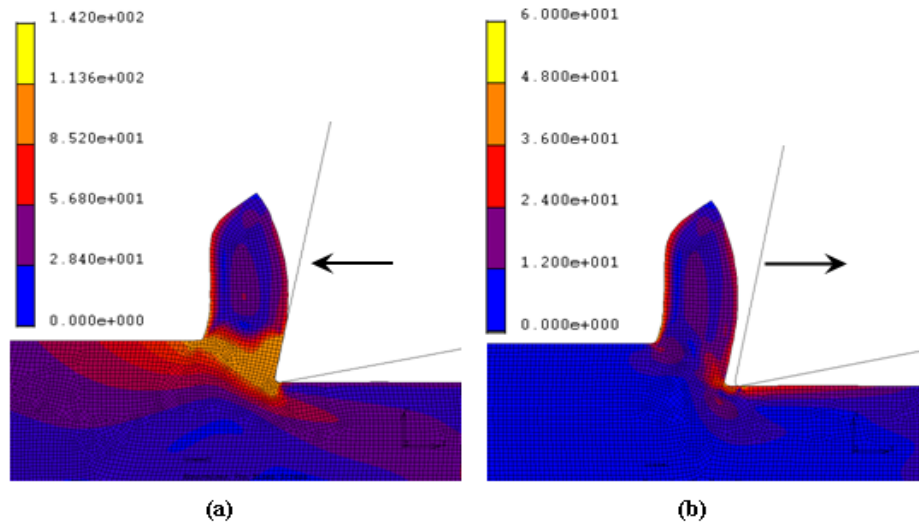


**Figure 3.** Distribution of von Mises (equivalent) stresses for a single cycle of ultrasonic vibration: (a) tool penetration. (b) tool moving away ( $f = 20$  kHz and  $a = 20$   $\mu\text{m}$ ). Duration of each cycle is 0.05 ms.

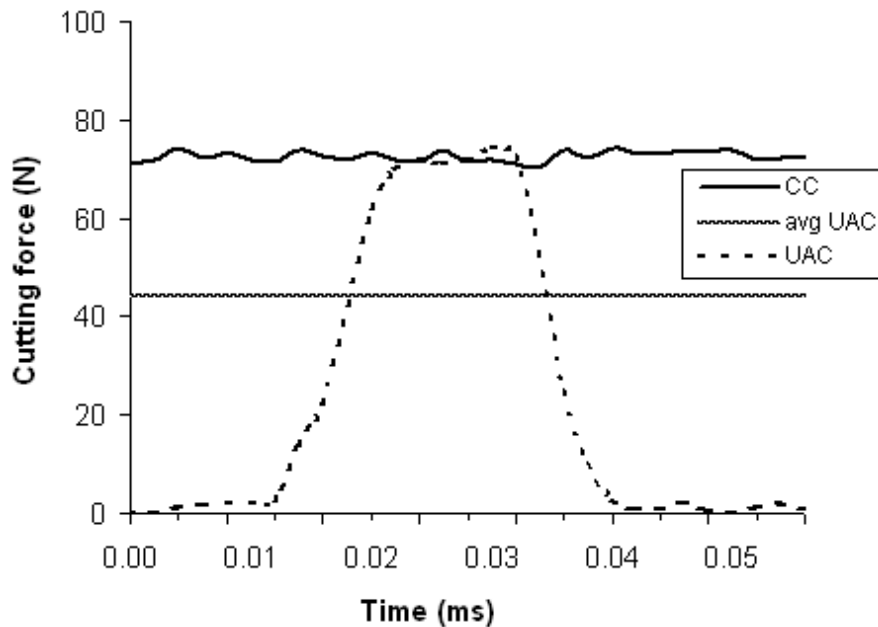


**Figure 4.** Comparison of calculated forces in cutting tool in simulations of CC and UAC. For UAC,  $f = 20$  kHz; and  $a = 20$   $\mu\text{m}$ .

the ultrasonic cycle, the average over a cycle stress developed in the bone material was considerably smaller than that in CC.

Comparison of forces in CC and UAC for the duration of one cycle is shown in figure 4. The average cutting force in UAC was calculated and its magnitude was approximately 40% lower than the respective magnitude for CC. For maximum penetration of the tool in the ultrasonic cycle, the level of stress induced in the material by the tool below its cutting tip (i.e. below the cut surface) decreased with increasing depth from the cut surface. The stress level is plotted in figure 5 against the depth.

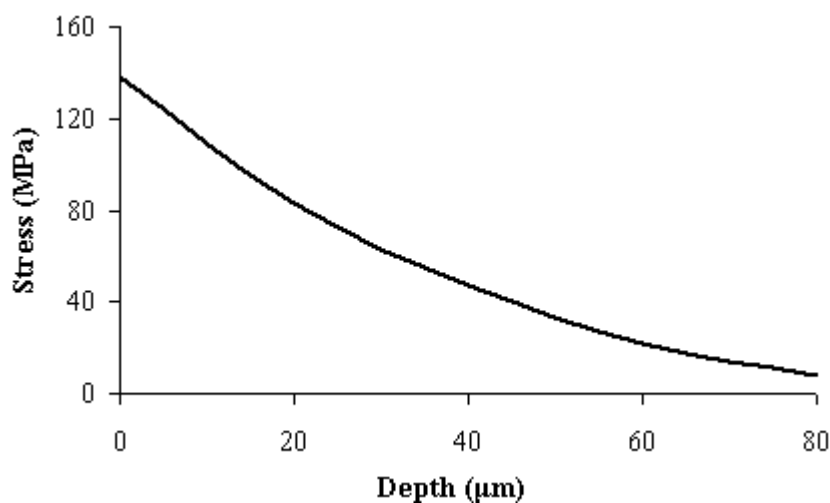


**Figure 5.** Variation of material stress with depth below the cut surface at the maximum tool penetration.  $f=20$  kHz and  $a = 20$  μm.

### 3.2 Effect of amplitude and frequency on stresses

To study the effect of amplitude of ultrasonic vibration on the stress developed in the bone material, the amplitude was varied between 10 and 30 μm (see table 3) while other parameters of UAC were kept constant. It was found that the amplitude of ultrasonic vibration did not influence the maximum stress magnitude. The maximum stress was achieved at the penetration depth of about 10 μm (for  $f=20$  kHz and  $a = 20$  μm) and remained nearly constant until the tool got the maximum displacement in the forward direction. For a constant frequency, the only effect of increasing amplitude was the increase in duration, for which the stress induced in the material retained its maximum magnitude. Changing ultrasonic frequency resulted in the speed at which the stress state changed in the material. The variation of cutting velocity was found to have no influence on peak stresses.

## 4. Conclusions

A 2D FE model was developed to simulate both conventional cutting (CC) and ultrasonically assisted cutting (UAC) of the bone material. The model is fully parametric and can simulate the cutting process for various cutting parameters, such as cutting velocity, tool's vibrational frequency and amplitude. The model allowed the study of chip formation predicting distributions of stresses and cutting forces in the bone material. Stress distributions in the cutting region were studied. When subjected to ultrasonic vibration, the material experienced a varying stress state depending on the motion and location of the tool in each cycle. The average stress level in the material using UAC was lower than that produced in CC.



## References

- [1] Harrysso O L, Hosni Y A and Nayfeh J F 2007 *BMC. Musculoskelet. Disord.* 8 91
- [2] Currey J D 1970 *J. Clin. Orthop. Relat. Res.* 73 210–31
- [3] Bonfield W 1987 *J. Biomech.* 20 1071–81
- [4] Norman T L, Vashishth D and Burr DB 1995 *J. Biomech.* 28 309–20
- [5] Zioupos P and Currey J D 1998 *Bone.* 22 57–66.
- [6] Yasuda Y, Noguchi, K and Sata T 1955 *J. Bone. Joint. Surg.* 37A 1292
- [7] Goodship A E, Lanyon L E and McFie H 1979 *J. Bone. Joint. Surg.* 61A 539
- [8] Tadano S and Todo M 1999 *IUTAM Symposium on Synthesis in Bio Solid Mechanics*, Kluwer Academic Publications 139-59
- [9] Tadano S and Okoshi T 2006 *J. Biomed. Mater. Eng.* 16(1) 11-21.
- [10] Mitsuishi M 2005 *Annals CIRP* 54 41-6
- [11] Lucas M, MacBeath A, McCulloch E and Cardoni A 2006 *Ultrasonics* 44 503–9.
- [12] Mitrofanov A V, Babitsky V I and Silberschmidt V V 2004 *J. Mat. Proc. Tech.* 153–54 233-239
- [13] Babitsky V, Kalashnikov A, Meadows and Wijesundara A 2003 *J. Mat. Proc. Tech.* 132 157-67
- [14] Astashev V K and Babitsky VI 1998 *Ultrasonics* 36 89-96
- [15] MSC. Marc User's Guide, Version 2007. MSC Software Corporation, Los Angeles
- [16] Naohiko S, Mamoru M, Yoshinori F and Tadaaki S 2006 *J. Jap. Soc. Adv. Prod. Tech.* 24 8-13
- [17] Mitsuishi M, Warisawa S and Sugita N 2004 *Annals CIRP* 53 107-12
- [18] Hortig C and Svendsen B 2007 *J. Mat. Proc. Tech.* 186 66–76
- [19] Huiskes J 1980 *Acta Orthop. Scandin., Suppl.* 185 44-108
- [20] Davidson S R H and James D F 2000 *Med. Eng. Phys.* 22(10) 741-47
- [21] Moses W M, Witthaus F W, Hogan H A and Laster W R 1995 *Exp. Therm. Fluid. Sci.* 11(1) 34-9